IL NUOVO CIMENTO VOL. 89 A, N. 1 1 Settembre 1985

Temperature and Free-Nucleon Densities of Nuclear Matter Exploding into Light Clusters in Heavy-Ion Collisions (*).

S. ALBERGO, S. COSTA, E. COSTANZO and A. RUBBINO

Dipartimento di Fisica dell'Università - Catania
Istituto Nazionale di Fisica Nucleare - Sezione di Catania
Centro Siciliano di Fisica Nucleare e di Struttura della Materia - Catania

(ricevuto l'1 Giugno 1985)

Summary. — A new statistical approach is adopted which, through a suitable analysis of light clusters emitted in heavy-ion collisions, allows us to evaluate temperature and free-nucleon densities of the emission source. All known data concerning the emission of ^{2}H, ^{3}H, ^{3}He, ^{4}He measured in a common experiment are used. These data refer to 19 heavy-ion reactions studied at projectile energies between 26 and 2100 MeV per nucleon. Analysed events are only those attributable to the equilibrium component through carefully adopted selections. Among the results, a correlation is observed between temperature T and total free-nucleon density ϱ_{t_F} of the emission source. A nuclear-matter model is formulated in order to compare its quantitative predictions with the observed (T, ϱ_{t_F}) correlation. A good agreement is found by this comparison.

PACS. 25.70. – Heavy-particle-induced reactions and scattering.

1. – Introduction.

The composite-particle emission, observed in intermediate- and high-energy heavy-ion interactions, is usually assumed to be the result of nuclear-matter explosion owing to near central collisions of the two interacting nuclei.

(*) To speed up publication, the authors of this paper have agreed to not receive the proofs for correction.

Several theoretical approaches to near central collisions of heavy ions have been made and a review of these models can be found in ref. [1-4]. Most of these theories have been concentrated on inclusive proton data.

The majority of adopted models assumes that a local equilibrium is reached either in the whole considered spaces, such as the phase space [5] and the interaction volume [6-12], or within particular subsystems. In these last cases, where few nucleons are involved, the local equilibrium is assumed within some peripheral nuclear regions in the « hot spot » model [13,14], or within the several tubes into which nuclei are divided in the « firestreak » model [15,16]. In the « coalescence » model [17-24] equilibrium between formation and break-up of composite fragments is assumed for nucleons located within the same coalescence p_0 radius centred at p in the momentum space.

Aim of this paper is to evaluate the temperature and the free-nucleon densities of equilibrated nuclear regions from which light fragments are emitted; more precisely, we evaluate the temperature and the free-nucleon densities of a piece of nuclear matter at the moment of its disassembly with a light-fragment emission, at large angles, not negligible with respect to free-nucleon emission.

---

(1) S. NAGAMIYA: *Proceedings of the Hakone Seminar, Hakone, July 1980,* edited by K. NAKAI and S. GOLDHABER, Vol. **1** (1980), p. 53.
(2) M. GYULASSY: *Proceedings of the Hakone Seminar, Hakone, July 1980,* edited by K. NAKAI and S. GOLDHABER, Vol. **1** (1980), p. 199.
(3) S. NAGAMIYA: *Proceedings of the V High Energy Heavy Ion Summer Study,* LBL-21652, Conf.-810504 (Berkeley, May 1981), p. 141.
(4) S. NAGAMIYA and M. GYULASSY: *Adv. Nucl. Phys.*, **13**, 201 (1984).
(5) J. RANDRUP and S. E. KOONIN: *Nucl. Phys. A*, **356**, 223 (1981).
(6) G. D. WESTFALL, J. GOSSET, P. J. JOHANSEN, A. M. POSKANZER, W. G. MEYER, H. H. GUTBROD, A. SANDOVAL and R. STOCK: *Phys. Rev. Lett.*, **37**, 1202 (1976).
(7) J. GOSSET, H. H. GUTBROD, W. G. MEYER, A. M. POSKANZER, A. SANDOVAL, R. STOCK and G. D. WESTFALL: *Phys. Rev. C*, **16**, 629 (1977).
(8) A. Z. MEKJIAN: *Phys. Rev. Lett.*, **38**, 640 (1977).
(9) A. Z. MEKJIAN: *Phys. Rev. C*, **17**, 1051 (1978).
(10) A. Z. MEKJIAN: *Nucl. Phys. A*, **312**, 491 (1978).
(11) A. Z. MEKJIAN: *Phys. Lett. B*, **89**, 177 (1980).
(12) S. DAS GUPTA and A. Z. MEKJIAN: *Phys. Rep.*, **72**, 131 (1981).
(13) R. WEINER and M. WESTRÖM: *Phys. Rev. Lett.*, **34**, 1523 (1975).
(14) R. WEINER and M. WESTRÖM: *Nucl. Phys. A*, **286**, 282 (1977).
(15) W. D. MYERS: *Nucl. Phys. A*, **296**, 177 (1978).
(16) J. GOSSET, J. I. KAPUSTA and G. D. WESTFALL: *Phys. Rev. C*, **18**, 844 (1978).
(17) S. T. BUTLER and C. A. PEARSON: *Phys. Rev. Lett.*, **7**, 69 (1961).
(18) S. T. BUTLER and C. A. PEARSON: *Phys. Lett.*, **1**, 77 (1962).
(19) S. T. BUTLER and C. A. PEARSON: *Phys. Rev.*, **129**, 836 (1963).
(20) A. SCHWARZSCHILD and C. ZUPANCIC: *Phys. Rev.*, **129**, 854 (1963).
(21) H. H. GUTBROD, A. SANDOVAL, P. J. JOHANSEN, A. M. POSKANZER, J. GOSSET, W. J. MEYER, G. D. WESTFALL and R. STOCK: *Phys. Rev. Lett.*, **37**, 667 (1976).
(22) H. MACHNER: *Phys. Lett. B*, **86**, 129 (1979).
(23) H. MACHNER: *Phys. Rev. C*, **21**, 2695 (1980).
(24) H. SATO and K. YAZAKI: *Phys. Lett. B*, **98**, 153 (1981).

To such a purpose, a statistical approach is adopted which makes use of all known data about the ^{2}H, ^{3}H, ^{3}He, ^{4}He cluster emission in heavy-ion collisions ([7,16,21,25-29]).

Among the several statistical models, only the coalescence ([17-24]) and the thermodynamic ([6-12]) models consider composite-particle emission. We adopt the thermodynamic picture since the information about the physical quantities we want here to evaluate may be gained by this model, which involves directly just the freeze-out temperature and nucleon density of the emitting source.

Thermal models, based on the assumption that the available energy is shared among interacting nucleons, may be justified when nucleon-nucleon $\mathcal{N}$-$\mathcal{N}$ collisions are dominant. More generally, the study of collective phenomena—such as compression, thermalization, hydrodynamical flow, equation of state, etc.—makes sense only if local equilibrium is reached through multiple $\mathcal{N}$-$\mathcal{N}$ collisions. Now, the emission of light clusters in a wide angular range just indicates multiple $\mathcal{N}$-$\mathcal{N}$ collisions. On this ground we adopt a statistical approach whose starting assumptions are the basic ones of the thermal model ([8-12]).

Since this model considers only a partial aspect of the complex reaction mechanism, it is important to restrict the analysis to those specific observables for which thermodynamics is likely to yield adequate results. Consequently, experimental data have been carefully analysed to select, among the components of the reaction mechanism, events attributable to the equilibrium component.

Among the results, a correlation is found between temperature and free-nucleon density. In order to give an interpretation of such an empirical result, a dilute-nuclear-matter model is proposed. Quantitative predictions of the model explain the observed correlation.

2. – Remarks.

2·1. *Uniqueness of evaporated composite particles to give information about the freeze-out stage.* – As first stage of reactions induced by heavy-ion collisions,

---

([25]) R. L. AULBE, J. B. BALL, F. E. BERTRAND, C. B. FULMER, D. C. HENSLEY, I. Y. LEE, R. L. ROBINSON, P. A. STELSON, C. Y. WONG, D. L. HENDRIE, H. D. HOLMGREN and J. D. SILK: *Phys. Rev. C*, **28**, 1552 (1983).

([26]) B. NEUMANN, H. REBEL, H. J. GILS, R. PLANETA, J. BUSHMANN, H. KLEWE-NEBENIUS, S. ZAGROMSKI, R. SHYAM and H. MACHNER: *Nucl. Phys. A*, **382**, 296 (1982).

([27]) G. D. WESTFALL, Z. M. KOENIG, B. V. JACAK, L. H. HARWOOD, G. M. CRAWLEY, M. W. CURTIN, C. K. GELBKE, B. HASSELQUIST, W. G. LYNCH, A. D. PANAGIOTOU, D. K. SCOTT, H. STÖCKER and M. B. TSANG: *Phys. Rev. C*, **29**, 861 (1984).

([28]) B. LUDEWIGT, G. GAUL, R. GLASOW, H. LÖHNER and R. SANTO: *Phys. Lett. B*, **108**, 15 (1982).

([29]) K. G. R. DOSS, H. A. GUSTAFSSON, H. H. GUTBROD, B. KOLB, H. LÖHNER, B. LUDEWIGT, A. M. POSKANZER, T. RENNER, H. RIEDESEL, H. G. RITTER, A. WARWICK and H. WIEMAN: GSI-85-4 Preprint (January 1985).

a hot interaction region may be created. This created hot region can reach, depending on the available energy in the c.m. frame:

a) Temperatures T not exceeding some tens of MeV, so that composite particles can be formed as a result of competitive processes.

b) Temperatures T much higher than the mean binding energy per nucleon. In this case the composite-particle production is strongly suppressed within the very hot region which may explode *either* b_1) through a complete disintegration in which free nucleons and pions are essentially emitted, *or* b_2) through two or several steps in which in the first stage only the hotter fraction of the nuclear region explodes with a dominating emission of free nucleons. Subsequently, within the remaining of the nuclear interaction system, cooled to lower temperatures, composite particles can be produced.

In both cases *a*) and b_2) the still hot nuclear system cools and expands. During this stage interactions are going on between the constituent particles until density and temperature become small enough so that the constituents are no longer interacting. From this time the particle composition remains unchanged (chemical freeze-out). As the system expands beyond that point, the frozen particles escape freely, by excluding only mutual Coulomb repulsion, until they are ultimately detected.

On these grounds, the evaporated composite particles, if suitably analysed, are unique in order to give information about the freeze-out stage which is the last stage in several heavy-ion interactions.

Instead, in order to deduce information about the initial stage of the reaction, well-defined assumptions must be made for the whole unknown and likely complex expansion phase.

2·2. *Nuclear-temperature evaluations.* – Before describing the procedure adopted in the present paper to evaluate temperature and free-nucleon densities of the considered piece of nuclear matter at the moment of its disassembly, let us shortly review and comment what is usually made to deduce the nuclear temperature.

The concept of temperature requires the existence of a local statistical equilibrium. Most of the authors consider, may be rightly, of dubious validity the assumption of such an equilibrium at densities close to or above the normal nuclear-matter density $\varrho_0 \simeq 0.15\ \mathrm{fm}^{-3}$.

However, in spite of such a disputable assumption, temperatures are usually evaluated by fitting exponential slopes of measured particle spectra with statistical treatments, which are, in principle, standard thermodynamic procedures. On the other hand, the experimental features of emitted-particle spectra resemble ordinary evaporation at large emission angles. This seems to give support to the assumption that the emission source may be approx-

imated as a piece of nuclear matter rather close to a thermal-equilibrium distribution.

To estimate the temperature T, the energy spectra $\mathcal{N}(E_{\text{c.m.}})$ in the c.m. rest frame of the emitting source are usually parametrized as

$$\mathcal{N}(E_{\text{c.m.}}) \propto E_{\text{c.m.}} \cdot \exp\left[-E_{\text{c.m.}}/T\right], \tag{1}$$

when a surface emission is assumed ([30,31]);

$$\mathcal{N}(E_{\text{c.m.}}) \propto E_{\text{c.m.}}^{\frac{1}{2}} \cdot \exp\left[-E_{\text{c.m.}}/T\right] \tag{1'}$$

within the assumption of a volume emission ([30,31]);

$$\mathcal{N}(E_{\text{c.m.}}) \propto \exp\left[-E_{\text{c.m.}}/T\right] \tag{1''}$$

when only the high-energy tails of the spectra are taken into account.

The values of T obtained by eqs. (1), (1'), (1'') can reach relative mutual deviations up to $(10 \div 20)\%$. Uncertainties of the order of 10% would be rather acceptable, but experimental data have to be transformed from the laboratory to the rest frame of the particular hypothesized emitting source. This transformation, which requires the use of several adjustable parameters, can give rise to large uncertainties in the T evaluations at intermediate energies. Actually, at intermediate energies, one can obtain very different T values by employing different combinations of the adopted parameters. For values of T comparable to the Coulomb barrier, relative deviations can reach values of about 100%. At higher energies, effects of the adjustable parameters become less and less critical at the increase of T. As, for instance, for values of $T \geqslant 50$ MeV, the relative deviations may reach maximum values of the order of 10%. On these grounds, extensive studies of temperature have been provided ([7,21,32]), at high energy, by fitting only the exponential tails of protons and π^- spectra for different target-projectile combinations. These high evaluated temperatures seem to saturate, up to beam energies of about 4 GeV/$\mathcal{N}$, at approximately $T_{\max} \simeq m_\pi c^2$, whose value is quite near to the limiting temperature predicted by HAGEDORN ([33]) and so far not definitively established ([34-36]).

([30]) A. S. GOLDHABER: *Phys. Rev. C*, **17**, 2243 (1978).

([31]) T. C. AWES, G. POGGI, C. K. GELBKE, B. B. BACK, B. G. GLAGOLA, H. BREUER and V. E. VIOLA jr.: *Phys. Rev. C*, **24**, 89 (1981).

([32]) S. NAGAMIYA, M.-C. LEMAIRE, E. MOELLER, S. SCHNETZER, G. SHAPIRO, H. STEINER and I. TANIHATA: *Phys. Rev. C*, **24**, 971 (1981).

([33]) R. HAGEDORN: *Suppl. Nuovo Cimento*, **3**, 147 (1965).

([34]) A. T. LAASANEN, C. EZELL, L. J. GUTAY, W. N. SCHREINER, P. SCHÜBELIN, L. VON LINDERN and F. TURKOT: *Phys. Rev. Lett.*, **38**, 1 (1977).

([35]) N. K. GLENDENNING and Y. KARANT: *Phys. Rev. Lett.*, **40**, 374 (1978).

([36]) H. STÖCKER, G. BUCHWALD, R. Y. ÇUSSON, G. GRAEBNER, W. GREINER, J. HOF-

3. – Analysis.

3·1. *Starting assumptions.* – We start with the assumption that a thermal equilibrium may be established between free nucleons and composite fragments contained within a certain interaction volume V at a temperature T. In the thermodynamic picture, the density $\varrho(A, Z)$ of a particle (A, Z) composed of Z bound protons and $A - Z$ bound neutrons may be expressed as follows:

$$\varrho(A, Z) = \frac{\mathcal{N}(A, Z)}{V} = \frac{A^{\frac{3}{2}} \cdot \omega(A, Z)}{\lambda_{T_{\mathcal{N}}}^3} \cdot F_{MB}\left[\frac{\mu(A, Z)}{T}\right], \tag{2}$$

where

$\mathcal{N}(A, Z)$ is the number of particles (A, Z) within the volume V;

$\lambda_{T_{\mathcal{N}}} = h/(2\pi m_0 T)^{\frac{1}{2}}$ is the thermal nucleon wave-length, where m_0 is the mass of a nucleon $\mathcal{N}$;

T is the temperature expressed in MeV;

$\mu(A, Z)$ is the chemical potential of the particle (A, Z);

$$\omega(A, Z) = \sum_j \{[2s_j(A, Z) + 1] \cdot \exp[- E_j(A, Z)/T]\} \tag{3}$$

is the internal partition function of the particle (A, Z), where $s_j(A, Z)$ are ground- and excited-state spins and $E_j(A, Z)$ are energies of these states;

$F_{MB}[\mu(A, Z)/T] = \exp[\mu(A, Z)/T]$ since we use the Maxwell-Boltzmann statistics. This because, for T larger than some MeV, provided that $\varrho < \varrho_0/2$, quantum statistics and boson condensation effects can be neglected for the light-cluster emission in heavy-ion collisions [37].

Now we impose to the considered thermodynamic system also the condition of chemical equilibrium, expressed by

$$\mu(A, Z) = Z\mu_{p_F} + (A - Z)\mu_{n_F} + B(A, Z), \tag{4}$$

where $B(A, Z)$ is the binding energy of the cluster (A, Z). μ_{p_F} and μ_{n_F} are the chemical potentials of free protons p_F and of free neutrons n_F, respectively.

MANN, H. KRUSE, J. A. MARUHN, B. MÜLLER, W. T. PINKSTON, P. R. SUBRAMANIAN, J. THEIS, D. VASAK, H. G. BAUMGARDT and E. SCHOPPER: *Proceedings of the International Conference on « Extreme States in Nuclear Systems », Dresden, February 4-9, 1980*, Vol. 2 (1980), p. 23.

[37] P. R. SUBRAMANIAN, L. P. CSERNAI, H. STÖCKER, J. A. MARUHN, W. GREINER and H. KRUSE: *J. Phys. G*, 7, L241 (1981).

From eqs. (2) and (4) it follows that

$$(5) \qquad \varrho(A, Z) = \frac{\mathcal{N}(A, Z)}{V} = \frac{A^{\frac{3}{2}} \lambda_{T,\mathcal{N}}^{3(A-1)} \omega(A, Z)}{(2s_{p_F} + 1)^Z (2s_{n_F} + 1)^{A-Z}} \varrho_{p_F}^Z \varrho_{n_F}^{A-Z} \exp\left[\frac{B(A, Z)}{T}\right],$$

$\varrho(A, Z)$, ϱ_{p_F} and ϱ_{n_F} being the densities of the composite (A, Z), of free protons and of free neutrons, respectively, contained in the same interaction volume V at the temperature T.

On the basis of such a thermodynamic picture the ratio $Y(A, Z)/Y(A', Z')$ between the experimental yields of two different emitted fragments is expected to be

$$(6) \qquad \frac{Y(A, Z)}{Y(A', Z')} = \frac{\varrho(A, Z)}{\varrho(A', Z')} = \left(\frac{A}{A'}\right)^{\frac{3}{2}} \left(\frac{\lambda_{T,\mathcal{N}}^3}{2}\right)^{A-A'} \frac{\omega(A, Z)}{\omega(A', Z')} \varrho_{p_F}^{Z-Z'} \varrho_{n_F}^{(A-Z)-(A'-Z')} \cdot \exp\left[\frac{B(A, Z) - B(A', Z')}{T}\right].$$

3·2. *Procedure to evaluate temperature and free-nucleon densities.* – Inspection of eq. (6) shows that the free-proton density of the emitting source at the moment of freeze-out can be easily obtained from the ratio between the experimental yields of two fragments differing only for a proton, such as (A, Z) and $(A + 1, Z + 1)$:

$$(7) \qquad \varrho_{p_F} = \left\{\left(\frac{A}{A+1}\right)^{\frac{3}{2}} \frac{10^{36}}{2.1} \frac{2s(A, Z) + 1}{2s(A+1, Z+1) + 1} T^{\frac{3}{2}} \cdot \exp\left[\frac{B(A, Z) - B(A+1, Z+1)}{T}\right]\right\} \frac{Y(A+1, Z+1)}{Y(A, Z)}.$$

Analogously, the yield ratio of two fragments differing only for one neutron such as (A, Z) and $(A + 1, Z)$ returns the free-neutron density:

$$(8) \qquad \varrho_{n_F} = \left\{\left(\frac{A}{A+1}\right)^{\frac{3}{2}} \frac{10^{36}}{2.1} \frac{2s(A, Z) + 1}{2s(A+1, Z) + 1} T^{\frac{3}{2}} \cdot \exp\left[\frac{B(A, Z) - B(A+1, Z)}{T}\right]\right\} \frac{Y(A+1, Z)}{Y(A, Z)}.$$

In eqs. (7) and (8), $\lambda_{T,\mathcal{N}}^3$ has been replaced by its value $4.2 \cdot 10^{-36} T^{-3}$ cm^3 with T expressed in MeV. The sum of $\omega(A, Z)$ (see eq. (3)) is limited to the ground state. This because the excitation energies $E_i(A, Z)$ of the here considered exploded isotopes of H and He are not significantly lower than temperatures expected to allow the composite-particle production (subsect. **2·1**). Then $\omega(A, Z)$ has been replaced by $2s(A, Z) + 1$, where $s(A, Z)$ is the ground-state spin.

So far, the majority of measured yields for composite-particle emission in heavy-ion collisions refers to light clusters. Then the present analysis is limited to the available experimental data on H and He isotope emission. The yield ratios between light clusters differing only for either a proton or a neutron we can use to deduce ϱ_{pF} and ϱ_{nF} are, in practice,

$$\frac{Y(^2\mathrm{H})}{Y(^1\mathrm{H})}, \quad \frac{Y(^3\mathrm{H})}{Y(^2\mathrm{H})}, \quad \frac{Y(^3\mathrm{He})}{Y(^2\mathrm{H})}, \quad \frac{Y(^4\mathrm{He})}{Y(^3\mathrm{H})}, \quad \frac{Y(^4\mathrm{He})}{Y(^3\mathrm{He})}.$$

In our analysis we exclude the ratio $Y(^2\mathrm{H})/Y(^1\mathrm{H})$ for the following reasons. Both in intermediate- and high-energy heavy-ion collisions, the energy spectra measured at large angles show exponentially decaying slopes as a function of the emitted-particle energy. These slopes are similar for the ^{2}H, ^{3}H, ^{3}He, ^{4}He energy spectra observed at the same angle and by using the same projectile-target combination at the same beam energy. This might indicate that these light composites have a common origin inside a source having a rather well-defined temperature. Instead the proton energy spectra may show quite different decreasing slopes. As, for instance, at lower energies, up to $\sim$20 MeV/$\mathcal{N}$ beams ([38]), the proton spectra slopes are less flat than the ones observed for light clusters. On the contrary, at higher energies, between 250 and 2100 MeV/$\mathcal{N}$ of the projectiles ([7]), the slopes of the proton spectra are flatter than those of the light-composite spectra. This seems to indicate that most of the protons are originated also within sources different from the common source of the emitted light clusters. Besides, the yields of light clusters are of the same order of magnitude at the same angle. Instead, the light cluster to proton ratios can vary, also by some orders of magnitude, as a function of the angle and of the energy per nucleon of the emitted particles ([39]). Consequently, very different evaluations of the ratio between light clusters and protons may be deduced by using data obtained within different angular ranges.

For these fundamental reasons we do not use the ratio $Y(\mathrm{d})/Y(\mathrm{p})$ for our evaluations. We use only the yield ratios between the light clusters ^{2}H, ^{3}H, ^{3}He, ^{4}He which, as a homogeneous group, seem to be good messengers of pieces of exploding nuclear matter at about the same temperature.

To use eqs. (7) and (8) we need to know the temperature T of the exploding piece of nuclear matter. To deduce this temperature we hypotesize a common origin for the exploded light nuclei which in our case range from deuterons to ^{4}He.

([38]) T. C. AWES, S. SAINI, G. POGGI, C. K. GELBKE, D. CHA, R. LEGRAIN and G. D. WESTFALL: *Phys. Rev. C*, **25**, 2361 (1982).

([39]) A. SANDOVAL, H. H. GUTBROD, W. J. MEYER, R. STOCK, CH. LUKNER, A. M. POSKANZER, J. GOSSET, C. JOURDAIN, C. H. KING, N. VAN SEN, G. D. WESTFALL and K. L. WOLF: *Phys. Rev. C*, **21**, 1321 (1980).

This assumption implies that, for a given temperature T of the emitting source, the same free-proton density must be evaluated by eq. (7), independently of the different used yield ratio. By using the quoted ratios, we obtain from eq. (7)

$$(9) \qquad \varrho_{p_F} = [0.39 \cdot 10^{36} T^{\frac{3}{2}} \exp[-5.5/T]] \frac{Y(^3\mathrm{He})}{Y(^2\mathrm{H})} = [0.62 \cdot 10^{36} T^{\frac{3}{2}} \exp[-19.8/T]] \frac{Y(^4\mathrm{He})}{Y(^3\mathrm{H})}.$$

Analogously, from eq. (8) concerning the free-neutron density, we obtain

$$(10) \qquad \varrho_{n_F} = [0.39 \cdot 10^{36} T^{\frac{3}{2}} \exp[-6.3/T]] \frac{Y(^3\mathrm{H})}{Y(^2\mathrm{H})} = [0.62 \cdot 10^{36} T^{\frac{3}{2}} \exp[-20.6/T]] \frac{Y(^4\mathrm{He})}{Y(^3\mathrm{He})}.$$

Equation (9), as well as eq. (10), yields

$$(11) \qquad T = \frac{14.3}{\ln\left[\frac{Y(^2\mathrm{H}) \cdot Y(^4\mathrm{He})}{Y(^3\mathrm{H}) \cdot Y(^3\mathrm{He})} \cdot 1.6\right]},$$

which requires only the knowledge of the complex yield ratio $Y(^2\mathrm{H}) \cdot Y(^4\mathrm{He}) / Y(^3\mathrm{H}) \cdot Y(^3\mathrm{He})$ to evaluate the temperature T.

At this point we can deduce the wanted quantities T, ϱ_{p_F} and ϱ_{n_F} by the following sequential procedure: first, we deduce the temperature T by means of eq. (11); then, this evaluated T value is used into eqs. (9) and (10) to obtain the densities of free protons ϱ_{p_F} and of free neutrons ϱ_{n_F}.

If now we introduce the quantity

$$x_{exp} = \frac{Y(^2\mathrm{H}) \cdot Y(^4\mathrm{He})}{Y(^3\mathrm{H}) \cdot Y(^3\mathrm{He})},$$

the maximum *a priori* relative uncertainty for the temperature T, easily deducible from eq. (11), can be expressed as

$$(12) \qquad \left|\frac{\mathrm{d}T}{T}\right| \simeq 7 \cdot 10^{-2} T \left|\frac{\mathrm{d}x}{x}\right|_{exp}.$$

Since $|\mathrm{d}T/T|$ increases linearly as a function of T, the more accurate estimates are obtained at lower temperatures, just where the usual T estimates, deduced by fitting the energy spectra, are affected by the largest uncertainties (subsect. 2·2).

On these grounds, the present method can be particularly appropriate to evaluate temperatures not exceeding some tens of MeV, as is just the case of nuclear regions which explode with emission of composite fragments too.

3·3. *Available energies per nucleon in the* c.m. *frame.* – The energy per nucleon of projectiles used in the experiments here considered ranges, in order of magnitude, from 10 to 10^3 MeV/$\mathcal{N}$ in the laboratory system. The portion of energy which can induce inelastic reactions is only that available in the c.m. frame.

In order to estimate, for each considered reaction, the mean energy per « participating » nucleon in the c.m. frame, we consider as « participating » the nucleons among which the largest amount of the available energy is actually distributed.

Let

A_p and A_T be the total number of projectile and target nucleons, respectively;

A_p^* and A_T^* be the « participating » nucleons of the projectile and of the target;

$(E/A_p)_{lab}$ be the energy per nucleon of the projectile in the laboratory system.

We can express the mean energy per « participating » nucleon in the c.m. frame $(E/(A_p^* + A_T^*))_{c.m.} = (E/A^*)_{c.m.}$, as follows:

$$\left(\frac{E}{A^*}\right)_{c.m.} = m_0 c^2 \left[\left(1 + \frac{2(A_T^*/A_p^*)\cdot(E/A_p)_{lab}}{(1 + A_T^*/A_p^*)^2 \cdot m_0 c^2}\right)^{\frac{1}{2}} - 1\right], \tag{13}$$

where $m_0 c^2$ is the nucleon rest energy.

A very large number of different energies per nucleon can be achieved, depending on the projectile and target nucleons actually interacting in the collision. To such a purpose we estimate the values of $(E/A^*)_{c.m.}$ under the following assumptions which encompass almost all the reasonable energy distributions among the colliding nucleons:

a) The available energy is shared among all target and projectile nucleons. In this case $A_T^*/A_p^* = A_T/A_p$ and within our assumptions the minimum value for $(E/A^*)_{c.m.}$ is obtained.

b) The projectile nucleons A_p interact essentially with about an equal number of target nucleons $A_T^* \simeq A_p$. In this case $A_T^*/A_p^* \simeq 1$ and, within the assumptions made, the maximum value of $(E/A^*)_{c.m.}$ is estimated.

For collisions between nuclei having nearly the same mass number $A_p \simeq A_T$ we have $A_T^*/A_p^* \simeq 1$, independently of the impact parameter.

3·4. *« Equilibrium » and « nonequilibrium » components.* – Since eqs. (9), (10) and (11) are based on the described equilibrium assumptions, we must consider only yields attributable to the equilibrium component of the whole reaction mechanism.

The spectral slopes are characterized by an exponential decrease *vs.* E, strongly suggesting evaporation processes, only at large transverse momenta ($\theta \geqslant (30 \div 40)^\circ$). But, at small emission angles, when the measured energy per nucleon E/A of the emitted particle A extends over a range which includes the projectile energy per nucleon E/A_p, the energy spectra of A can exhibit broad peaks at energies slightly less than E/A_p. This fact suggested a projectile fragmentation resulting from peripheral nucleus-nucleus collisions. The first interpretations of the fragmentation have been given by FESHBACH and HUANG ([40-42]) and by GOLDHABER ([43]), by relating the widths of the momentum distributions observed in the fragmentation peaks to the intrinsic nucleon Fermi motion inside the projectile. Their models, developed for the projectile fragmentation at relativistic energies ([44,45]), are to day applied to explain also the very similar projectile fragmentation observed at lower energies down to some tens of MeV/$\mathcal{N}$ ([25,31,46,47]).

At intermediate energies $E/A_p \lesssim 200$ MeV/$\mathcal{N}$ and at forward angles, the energy spectra of emitted particles A, usually measured up to $E/A \simeq 200$ MeV/$\mathcal{N}$, include both the evaporation and the fragmentation contributions. At small angles and in the rest frame of the projectile fragment, the Gaussian momentum distribution is given by ([45-48])

$$\mathcal{N}(\boldsymbol{p}_A) \propto \exp\left[-\boldsymbol{p}_A^2/2\sigma_\parallel^2\right] = \exp\left[-(\boldsymbol{p}_{A_p} - \langle \boldsymbol{p}_\parallel \rangle)^2/2\sigma_\parallel^2\right], \tag{14}$$

where

A and A_p are the mass number of fragment and projectile, respectively;

$\langle p_\parallel \rangle$ is the displacement from the projectile momentum;

([40]) H. FESHBACH and K. HUANG: *Phys. Lett. B*, **47**, 300 (1973).
([41]) K. HUANG: *Phys. Rev.*, **146**, 1075 (1966).
([42]) K. HUANG: *Phys. Rev.*, **156**, 1555 (1967).
([43]) A. S. GOLDHABER: *Phys. Lett. B*, **53**, 306 (1974).
([44]) H. H. HECKMANN: *Proceedings of the V International Conference on High Energy Physics and Nuclear Structure, Upssala, June 1973*, LBL-2052 (1973).
([45]) D. E. GREINER, P. J. LINDSTROM, H. H. HECKMANN, B. CORK and F. S. BIESER: *Phys. Rev. Lett.*, **35**, 152 (1975).
([46]) C. K. GELBKE, D. K. SCOTT, M. BINI, D. L. HENDRIE, J. L. LAVILLE, J. MAHONEY, M. C. MERMAZ and C. OLMER: *Phys. Lett. B*, **70**, 415 (1977).
([47]) J. B. NATOWITZ, M. N. NAMBOODIRI, L. ADLER, R. P. SCHMITT, R. L. WATSON, S. SIMON, M. BERLANGER and R. CHOUDHURY: *Phys. Rev. Lett.*, **47**, 1114 (1981).
([48]) G. D. WESTFALL, R. G. SEXTRO, A. M. POSKANZER, A. M. ZEBELMAN, G. W. BUTLER and E. K. HYDE: *Phys. Rev. C*, **17**, 1368 (1978).

the width $\sigma_{0\parallel}$, independent of the observed fragment, is connected to the standard deviation $\sigma_\parallel$, to the temperature T and to the nucleon Fermi momentum p_F inside the projectile by ([43,45-47])

$$\sigma_{0\parallel}^2 = \sigma_\parallel^2 \frac{A_p - 1}{A(A_p - A)} \simeq m_0 T \frac{A_p - 1}{A_p} \simeq \frac{p_F^2}{5}, \tag{15}$$

where m_0 is the nucleon mass.

The corresponding kinetic-energy spectrum becomes just a Maxwellian distribution of the form

$$\mathcal{N}(E_A) \propto \sqrt{E_A} \exp[-E_A/T]. \tag{16}$$

Then, the energy spectra of the projectile fragments simulate an evaporation emission from a compound nucleus.

Consequently, the measured energy spectra of particles emitted at forward angles in intermediate-energy heavy-ion collisions are to be assumed as the sum of, at least, two different Maxwell-Boltzmann distributions.

In order to separate the equilibrium component from the nonequilibrium components, we roughly divide the several reaction contributions into two categories:

a) *Equilibrium component*, essentially concerning central collisions, and more generally fusionlike reactions, characterized by a source having a velocity not higher than about half that of the projectile. The particle emission due to this component covers the whole angular range and the energy spectra exhibit exponential slopes decreasing *vs.* E.

b) *Nonequilibrium component*, predominantly arising from peripheral projectile fragmentation associated to break-up, and more generally to transferlike reactions, with emitted particles having about the projectile velocity. The light-fragment A emission due to this component is essentially localized at small forward angles and at energies per nucleon E/A close to the energy per nucleon E/A_p of the projectile.

3·5. *Treatment of experimental data.* – In order to use the evaluation method described in subsect. **3**·2, we need

the experimental complex yield ratio $Y(^2\mathrm{H}) \cdot Y(^4\mathrm{He})/Y(^3\mathrm{H}) \cdot Y(^3\mathrm{He})$ to evaluate T by means of eq. (11);

the measured single yield ratios, either $Y(^4\mathrm{He})/Y(^3\mathrm{H})$ or $Y(^3\mathrm{He})/Y(^2\mathrm{H})$, to evaluate ϱ_{p_F} according to eq. (9);

the measured single yield ratios, either $Y(^4\mathrm{He})/Y(^3\mathrm{He})$ or $Y(^3\mathrm{H})/Y(^2\mathrm{H})$, to evaluate ϱ_{n_F} according to eq. (10).

TABLE I.

References	1	2	3	4	5	6		7	8	9
	Projectile	Target	E/A_p (MeV)	Measured E_{min} (MeV)	θ_{lab}	$(E/A^*)_{c.m.}$ (MeV/$\mathcal{N}$) min	max	T (MeV)	ϱ_{pF} (10^{35}/cm^3)	ϱ_{nF} (10^{35}/cm^3)
(26)	^{6}Li	^{40}Ca	26	$\sim 5A$	15°, 20°	2.9	6.5	4.1	1.4	2.0
(27)	^{12}C	^{197}Au	35	$\sim 5A$ (H), $\sim 7A$ (He)	(40÷140)°	1.9	8.7	4.6	1.2	5.0
(28)	^{4}He	^{58}Ni	43	~ 20	55°	2.6	10.7	5.0	5.4	3.8
(28)	^{4}He	^{197}Au	43	~ 20	55°	0.84	10.7	4.3	1.0	4.2
(25)	^{16}O	Ni	51.8	$\sim 10A$ (H), $\sim 15A$ (He)	(6÷155)°	8.7	12.9	4.0	1.5	1.7
(25)	^{16}O	^{27}Al	100	$\sim 10A$ (H), $\sim 15A$ (He)	(6÷155)°	23.1	24.7	6.1	5.5	5.5
(25)	^{16}O	Ni	100	$\sim 10A$ (H), $\sim 15A$ (He)	(6÷155)°	16.7	24.7	6.0	5.8	5.8
(25)	^{16}O	Sn	100	$\sim 10A$ (H), $\sim 15A$ (He)	(6÷155)°	10.4	24.7	5.9	3.6	5.6
(25)	^{16}O	^{197}Au	100	$\sim 10A$ (H), $\sim 15A$ (He)	(6÷155)°	6.9	24.7	5.5	2.7	4.6
(25)	^{16}O	Ni	147	$\sim 10A$ (H), $\sim 15A$ (He)	(6÷155)°	24.4	36.1	7.6	7.9	8.8
(25)	^{16}O	^{197}Au	147	$\sim 10A$ (H), $\sim 15A$ (He)	(6÷155)°	10.2	36.1	7.4	5.9	10.5
(7)	^{4}He	^{238}U	400	$\sim 25A$ (H), $\sim 30A$ (He)	60°, 90°	6.5	95	8.5	14	31
(7,21)	^{20}Ne	^{238}U	250	$\sim 25A$ (H), $\sim 30A$ (He)	60°, 90°	17.7	60	8.7	16	25
(7,21)	^{20}Ne	^{238}U	400	$\sim 25A$ (H), $\sim 30A$ (He)	60°, 90°	28.2	95	10.0	22	40
(16)	^{20}Ne	^{238}U	2100	$\sim 25A$ (H), $\sim 30A$ (He)	60°, 90°	140	427	12.2	60	55
(29)	^{93}Nb	^{93}Nb	400	$12A$	(9÷160)°	95		14.4	41	74
(29)	^{93}Nb	^{93}Nb	650	$12A$	(9÷160)°	150		15.3	48	102
(29)	^{40}Ca	Ca	400	$12A$	(9÷160)°	95		13.9	39	51
(29)	^{40}Ca	Ca	1050	$12A$	(9÷160)°	233		16.5	76	88

The emission of the four fragments ^{2}H, ^{3}H, ^{3}He, ^{4}He, measured in a common experiment, has been studied for the heavy-ion reactions ([7,16,21,25-29]) reported in table I. The first 5 columns of the table summarize some experimental data for these reactions.

To evaluate T, ϱ_{pF} and ϱ_{nF}, corrections to some of the measured yields are necessary, because

a) the experimental yields of ref. ([25,26]) include the contribution due to projectile fragmentation,

b) the minimum detected energies in ref. ([7,16,21]) are so large that remarkable fractions of the evaporated particles are lost.

For these cases we describe in detail the applied corrections.

Reference ([26]). Data used in our analysis are deduced by subtracting from experimental spectra at $\theta_{lab} = 15°$ and $20°$ the elastic plus inelastic transfer contributions according to evaluations made in the same ref. ([26]).

Reference ([25]). The measured spectra include, at small angles, a remarkable contribution from the transferlike peripheral reactions. A two-component model is adopted ([25]) and the cross-sections in terms of the momentum distributions are expressed as a sum of two independent contributions classified as σ_c for « central collisions » and σ_t for « peripheral fragmentations ».

The values of σ_c and σ_t are deduced ([25]) by fitting the inclusive experimental spectra in the following cases:

^{2}H and ^{4}He for all the studied reactions,

^{3}He for the ^{16}O+Ni reactions only,

for ^{3}H σ_c and σ_t are not deduced.

The procedure adopted in the present paper in order to evaluate T, ϱ_{pF} and ϱ_{nF} needs the knowledge of the emission yields of all the four evaporated fragments ^{2}H, ^{3}H, ^{3}He, ^{4}He. Then, we cannot directly use the obtained ([25]) σ_c values into our eqs. (9)-(11) because of the lack of these values for the ^{3}H emission and because of the partial availability of σ_c for the ^{3}He emission. However, in spite of this partial lack of data about σ_c, we think it possible to estimate indirectly this quantity. Such a possibility is based on the following two grounds:

a) the total yields of the four fragments ^{2}H, ^{3}H, ^{3}He, ^{4}He are measured for all the seven studied reactions and their values are summarized in table III of ref. ([25]);

b) the ratio $\sigma_c/(\sigma_c + \sigma_t)$, which represents the fraction of the total cross-section attributed to the « central collisions », is limited ([25]) to within 0.73 ± 0.05 for ^{2}H and within 0.46 ± 0.05 for ^{3}H, independently of the projectile energy

(51.8, 100 and 147 MeV/$\mathcal{N}$). Instead, for ^{4}He, the ratio $\sigma_c/(\sigma_c + \sigma_f)$ decreases *vs.* the projectile energy and the found ([25]) values are limited to within $0.20 \pm \pm 0.02$ at 147 MeV/$\mathcal{N}$, 0.31 ± 0.06 at 100 MeV/$\mathcal{N}$ and ~ 0.5 at 51.8 MeV/$\mathcal{N}$.

In order to deduce the emission yields attributable to the equilibrium component, we multiply the total measured yields ([25]) by the corresponding ratio $\sigma_c/(\sigma_c + \sigma_f)$ for each of the four considered fragments. For the ^{3}He emission we assume a ratio $\sigma_c/(\sigma_c + \sigma_f)$ equal to that found for the ^{3}H emission.

References ([7,16,21]). The maximum measured ([7,16,21]) energy per nucleon of emitted light clusters does not exceed ~100 MeV/$\mathcal{N}$. Thus the observed energy spectra do not include the fragmentation peak and they exhibit, also at small angles, only the decreasing exponential shape, characteristic of evaporation processes. But, since the minimum detected energies ([7,16,21]) are $\sim 25\,A$ for ^{2}H and ^{3}H and $\sim 30\,A$ for ^{3}He and ^{4}He, a large fraction of evaporation yields is lost. Besides, such a lost fraction is different for the different clusters. For

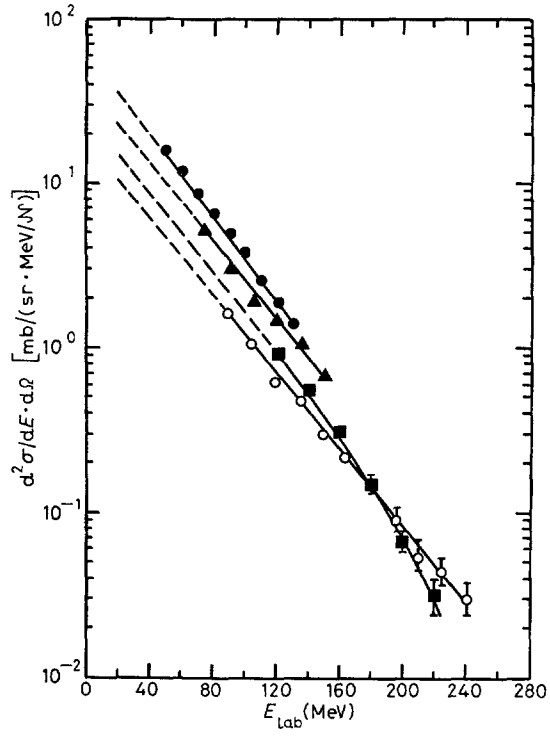

Fig. 1. – Example of the energy spectra extrapolation (dashed part of the lines) here adopted in the low-energy region for data of ref. ([7,21]). Shown data are those measured at $\theta_{lab} = 90°$ in the reaction ^{20}Ne+U at $(E/A_p)_{lab} = 250$ MeV/$\mathcal{N}$ and refer to the ^{2}H (•), ^{3}H (▲), ^{3}He (○), ^{4}He (■) emission. In the abscissa axis, the energy per nucleon reported by the authors ([7,21]) has been transformed into the total measured energy of emitted light clusters.

these reasons we extrapolate the spectra measured at $\theta_{lab} = 60°$ and $90°$ in the low-energy region. An example of such an extrapolation is shown in fig. 1.

We evaluate the yield ratios by extrapolating the spectra down to minimum values $E_{min} = 20, 30$ and 40 MeV. Mutual relative deviations of the temperatures calculated by using into eq. (11) the yields deduced by spectra extrapolated in these three different ways are lower than $\sim 6\,\%$.

Reference ([29]). Experimental data of ref. ([29]) exclude the contributions from the target and projectile spectators. Ratios of the emitted particles to protons are given ([29]) as functions of the charge multiplicity N_p with N_p ranging up to ~ 40 for ^{40}Ca+Ca and up to ~ 80 for ^{93}Nb+^{93}Nb. Yields used by us are those measured ([29]) at $N_p = 20, 25, 30, 35$ for ^{40}Ca+Ca and $N_p = 30, 40, 50, 60, 70$ for ^{93}Nb+^{93}Nb. The several values of T deduced for each reaction at the several values of N_p agree with each other within about 15 %.

4. – Results.

By using the procedure described in sect. **3** we evaluate the temperature T, the free-nucleon densities ϱ_{p_F} and ϱ_{n_F}, the minimum and the maximum values of the available energy per nucleon $(E/A^*)_{c.m.}$ in the c.m. frame.

Results of these evaluated quantities are summarized in the last 4 columns of table I. Some features of these results are discussed in the following subsections.

4·1. *Free-nucleon densities.* – To date evaluations made about the nucleon densities essentially concern the following two aspects:

a) According to the approximate relationship

$$\frac{\varrho_{n_F}}{\varrho_{p_F}} \simeq \frac{Y(^3\mathrm{H})}{Y(^3\mathrm{He})}, \tag{17}$$

estimates have been made of the ratio between these two densities by the knowledge of the experimental ratio $Y(^3\mathrm{H})/Y(^3\mathrm{He})$ (see, for instance, ref. ([32])). By such an analysis no estimates can be deduced about the absolute values of the nucleon densities. From our results, which give the absolute values of ϱ_{p_F} and ϱ_{n_F}, we can deduce as secondary product the ratios $\varrho_{n_F}/\varrho_{p_F}$. Values of these ratios here obtained exhibit, in agreement with known data ([32]), a general trend increasing *vs.* the ratio N/Z, where N and Z are neutron and proton numbers of the target plus projectile system.

b) Due to its connection with the entropy per nucleon according to the

usually adopted relationship ([30,31,32,49-51])

$$S_1 = 3.95 - \ln\left[\frac{Y(\mathrm{d})}{Y(\mathrm{p})}\right], \tag{18}$$

the ratio $Y(\mathrm{d})/Y(\mathrm{p})$ has been extensively studied. The knowledge of the ratio $Y(\mathrm{d})/Y(\mathrm{p})$ could allow, in principle, the estimation of ϱ_{n_F} through, for instance, eq. (8) if the temperature T is known. But on this subject we have to recall, as pointed out in subsect. 3·2, that, among the $Y(A+1)/Y(A)$ ratios, the $Y(\mathrm{d})/Y(\mathrm{p})$ one should be the less suitable ratio to be used for such a purpose.

Usually the measured yield ratios $Y(\mathrm{d})/Y(\mathrm{p})$ are used directly into eq. (18) to evaluate the entropy. In order to explain discrepancies between theory and experiments concerning S_1, it is sometimes suggested that the nucleon density should be very small (see, for instance, ref. ([31,32])).

As a matter of fact, a lack of data is found about the evaluated values of free-nucleon densities, especially for dilute nuclear matter. In this situation we cannot compare our evaluated absolute values of the free-nucleon densities with other evaluations.

4·2. *Temperature.* – The here evaluated temperatures are always lower than the maximum energy per nucleon available in the c.m. frame. This remark seems to be rather obvious, but the condition $T < [(E/A^*)_{\mathrm{c.m.}}]_{\max}$ is sometimes not satisfied for temperatures evaluated by fitting the energy spectra of emitted particles at intermediate projectile energies. This might be due to the fact that the unavoidable use of several adjustable parameters can strongly influence such T evaluations at intermediate energies, as pointed out in subsect. 2·2.

Now we consider the 7 reactions studied in the common experiment described in ref. ([25]). Temperatures evaluated by selecting yields attributable to the «equilibrium component», given in table I, are reported in fig. 2*a*) as a function of the projectile laboratory energy per nucleon. Besides we evaluate, for these 7 cases, the yields attributable to the «nonequilibrium component». Following the treatment of data described in subsect. 3·5 we multiply, this time, the total measured yields by the ratio $\sigma_t/(\sigma_e + \sigma_t)$. Yields so selected are used in eq. (11) to evaluate the temperatures T_p associated to the hypothetical projectile decays. In fig. 2*b*) these T_p evaluations, reported *vs.* $(E/A_p)_{\mathrm{lab}}$, are compared with the dashed straight line which corresponds to a constant temperature $T = 7.3$ MeV.

([49]) P. J. SIEMENS and J. I. KAPUSTA: *Phys. Rev. Lett.*, **43**, 1486 (1979).
([50]) H. STÖCKER, G. BUCHWALD, G. GRAEBNER, P. SUBRAMANIAN, J. A. MARUHN, W. GREINER, B. V. JACAK and G. D. WESTFALL: *Nucl. Phys. A*, **400**, 63c (1983).
([51]) J. KAPUSTA: *Phys. Rev. C*, **29**, 1735 (1984).

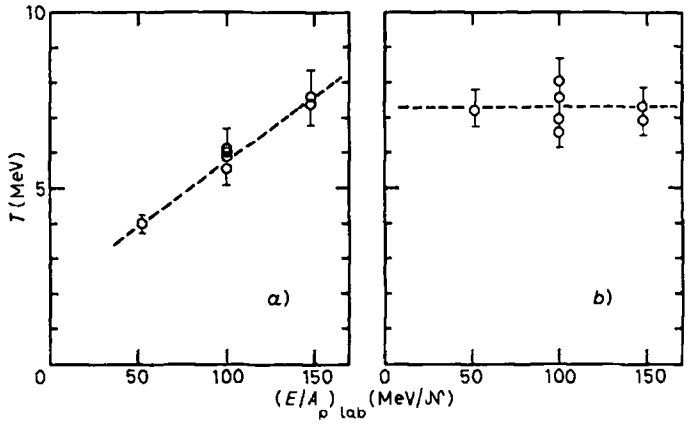

Fig. 2. – Temperatures *vs.* the projectile laboratory energy per nucleon here evaluated for the seven reactions studied in ref. ([25]) by selecting events attributable *a*) to the equilibrium component, *b*) to the projectile fragmentation.

By analysing the momentum Gaussian distributions of the fragmentation component, the authors of ref. ([25]) deduce for $A = 2 \div 4$ a value $\sigma_{0\parallel} = (80 \pm \pm 5)$ MeV/c for all the 7 studied reactions. This result, according to eq. (15), corresponds to $T = (7.3 \pm 1)$ MeV. Then, T_p values deduced by means of the present approach, which makes a suitable use of selected yield ratios, are in excellent agreement with the temperatures evaluated ([25]) by the momentum distributions of the fragmentation component.

We underline that the value $T = 7.3$ MeV, which corresponds in the fragmentation picture to an equivalent excitation temperature, is remarkably close to the mean nucleon binding energy, as expected. In fact, the T_p are related to the projectile intrinsic nucleon Fermi momentum p_F through eq. (15) and their values are also expected to be independent of the projectile energies E/A_p.

On the contrary, the temperatures T concerning the « equilibrium component » exhibit an increasing trend *vs.* E/A_p, as shown by the dashed straight line of fig. 2*a*).

4·3. *Correlation between total free-nucleon density and temperature.* – In fig. 3 we report the total free-nucleon density $\varrho_{t_F} = \varrho_{p_F} + \varrho_{n_F}$ as a function of the temperature T. The behaviour of the points which represent the (T, ϱ_{t_F}) pairs seems to suggest that ϱ_{t_F} can be approximated as proportional to T^3, at least within the whole range covered by the found T values ($T \sim (4 \div 20)$ MeV). Under this empirical assumption, points of fig. 3 are fitted by the full straight line drawn in the figure, which represents the equation

$$\varrho_{t_F} = 5.3 \cdot 10^{33} T^3 \ (\mathrm{cm}^{-3}) \,. \tag{19}$$

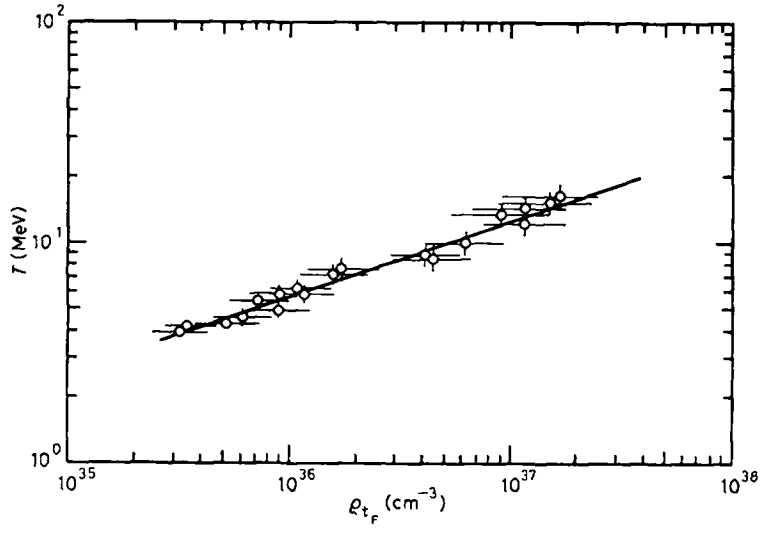

Fig. 3. – Open circles represent evaluated total free-nucleon density $\varrho_{t_F} = \varrho_{p_F} + \varrho_{n_F}$ as a function of the temperature T. The full straight line shows the T-dependence of ϱ_{t_F} according to eq. (19).

We shall formulate a model of dilute nuclear matter in order to deduce an approximate but quantitative interpretation of this correlation.

5. – Interpretation of the (T, ϱ_{t_F}) correlation.

5·1. *Dilute-nuclear-matter model.* – The constituents of the dilute-nuclear-matter system are free nucleons and composite particles. Experimental data indicate that the number of free nucleons with respect to the number of composite particles is in every case large enough to allow the assumption that the density of free nucleons ϱ_{t_F} is comparable to the density of all constituents ϱ_t.

At values of $T \leqslant 20$ MeV, the composite particles are much more immune from mutual inelastic interactions, with respect to free nucleons which can still suffer inelastic collisions. This means that, at moderate values of T, the majority of interactions which can modify the constituent composition are those induced by free nucleons. This picture is consistent with the fact that the ratio between bound and free nucleons increases at the decrease of T.

On this basis we consider only inelastic interactions induced by free nucleons within the dilute-nuclear-matter system; besides, we assume that interactions between a free nucleon and another nucleon, either free or bound in light clusters, may be described by adopting the same interaction potential for free as well as for bound nucleons.

Recently, some authors ([52-55]) have pointed out that the potential binding energy $U(r)$, as a function of the interparticle separation distance r, obeys a «universal» relation for several considered particles such as atoms, molecules and nucleons. Different physical phenomena, concerning different systems—atomic ([52]), molecular ([52]), metallic ([52-54]) and nuclear ([55]) systems—have been described in terms of the same binding-energy–distance relation:

$$U(r) = \Delta U \cdot U^*(r^*), \tag{20}$$

where

$r^* = (r - r_0)/l$;

$U^*(r^*)$ is a «universal function» ([52-55]) which for nuclear systems is expressed in the approximate form ([55]) $U^*(r^*) = -(1 + r^*)\exp[-r^*]$;

ΔU is a scaling parameter which represents the equilibrium binding energy;

r_0 is the equilibrium spacing;

r is the separation distance of nucleons;

l is a length scale, defined by $l = [\Delta U/(\mathrm{d}^2 U/\mathrm{d}r^2)_{r_0}]^{\frac{1}{2}}$.

Among several investigations about $U(r)$, a very recent study of the radial and energy dependence of $U(r, E)$ has been extensively made ([56]) to describe interactions between nucleons and even-even nuclei with $A = 2Z = 2N$.

The potential energy $U(r)$ for nuclear matter is currently expressed also in the form of a power series of the density $\varrho/\varrho_0 \simeq (r_0/r)^3$. $\varrho_0 \simeq 0.15$ nucleons/fm^3 is the saturation density. A representative example of this form is that recently proposed by KAPUSTA ([51]):

$$U(\varrho) = \sum_{i=2}^{5} a_i (\varrho/\varrho_0)^{i/3}. \tag{21}$$

The comparison between trends of $U(r)$ according to eqs. (20) and (21), made in ref. ([55]), shows very similar trends of these two adopted forms.

In the following we will use for $U(r)$ eq. (20) which, in terms of only two parameters, describes the zero-temperature binding energy as a function of the separation between nucleons.

([52]) J. FERRANTE, J. R. SMITH and J. H. ROSE: *Phys. Rev. Lett.*, **50**, 1385 (1983).
([53]) J. H. ROSE, J. R. SMITH and J. FERRANTE: *Phys. Rev. B*, **28**, 1835 (1983).
([54]) J. H. ROSE, J. R. SMITH, F. GUINEA and J. FERRANTE: *Phys. Rev. B*, **29**, 2963 (1984).
([55]) J. H. ROSE, J. P. VARY and J. R. SMITH: *Phys. Rev. Lett.*, **53**, 344 (1984).
([56]) A. PASCOLINI and C. VILLI: *Nuovo Cimento A*, **85**, 89 (1985).

The total energy-distance relation for monoenergetic nucleons with kinetic energy E would be

$$E_t(r) = U(r) + E\,. \tag{22}$$

5·2. *Nucleon capture interactions.* – We consider now capture interactions between nucleons. A colliding nucleon remains unbound for

$$U(r) + E > 0\,, \tag{23}$$

while it is captured in a bound state for

$$U(r) + E < 0\,. \tag{23'}$$

The condition

$$U(r) + E = 0 \tag{23''}$$

establishes, for each value of $E < \Delta U$, the corresponding radial distance $[r_{NC}(E)]_{\Delta U}$ below which the colliding nucleon is captured.

The nucleon capture cross-section for monoenergetic nucleons can be estimated, as a function of the capture radius $[r_{NC}(E)]_{\Delta U}$, by

$$[\sigma_{NC}(E)]_{\Delta U} \simeq \pi [r_{NC}(E)]^2_{\Delta U}\,. \tag{24}$$

Now we have to take into account that, according to the model assumptions, thermalyzed nucleons have a Maxwell-Boltzmann energy distribution. Thus we define a capture radius $[r_{NC}(T)]_{\Delta U}$, depending this time on T, as the weighted average of the capture radius $[r_{NC}(E)]_{\Delta U}$ over the Maxwell-Boltzmann distribution $P(E)$, that is,

$$[r_{NC}(T)]_{\Delta U} = \int_{\sim 0}^{\Delta U} [r_{NC}(E)]_{\Delta U} P(E)\, \mathrm{d}E\,, \tag{25}$$

where

$$P(E) = 2\pi^{-\frac{1}{2}} T^{-\frac{3}{2}} E^{\frac{1}{2}} \exp\left[-E/T\right]. \tag{26}$$

In this way, the nucleon capture cross-section as a function of T can be evaluated as

$$[\sigma_{NC}(T)]_{\Delta U} \simeq \pi [r_{NC}(T)]^2_{\Delta U}\,. \tag{27}$$

We consider (subsect. **5·1**) only inelastic interactions induced by free nucleons by assuming (subsect. **5·1**) that interactions of a free nucleon with either free or bound nucleons can be described by the same potential. Then values

used for the potential parameters r_0 and ΔU to calculate $[r_{NC}(T)]_{\Delta U}$ are independent of the fact that the free nucleon interacts with either a free or a bound nucleon.

For the equilibrium spacing r_0 we use the fixed reasonable value, often adopted, $r_0 \simeq 1.1$ fm ([55]) since only small deviations from this value are allowed.

Currently adopted values for the equilibrium binding energy ΔU range from 16 MeV ([55]), concerning infinite nuclear matter, to 8 MeV ([51]), when surface effects in finite nuclei are taken into account. This range is large enough to encompass also interactions between free nucleons and bound nucleons. Then, also in account of the fact that the density of composite particles is negligible with respect to the density of free nucleons (subsect. 5·1), we think that the use of a common value for ΔU cannot significantly alter the evaluation of the quantities we will deduce in the next subsection.

5·3. *Comparison of the* (T, ϱ_{t_F}) *correlation with predictions of the model* – Now we define within the expanding system, which represents also the emission source, the following quantities:

A_F^*, total number of free nucleons;

Φ and V, linear dimensions and volume, respectively, of the source whose expansion is assumed to be nearly isotropic so that $\Phi^3 \simeq 2V$;

$k = \varrho_t/\varrho_{t_F}$, ratio between the density of all constituents and the density of free nucleons;

$L_{NC} = 1/\varrho_t[\sigma_{NC}(T)]_{\Delta U}$, nucleon mean free path against nucleon captures as a function of temperature;

$a = L_{NC}/\Phi$, parameter related to the probability P_{NF} that a nucleon does not suffer capture collisions by $P_{NF} = \exp[-1/a]$. The freeze-out conditions depend on this probability.

A correlation between these quantities yields

$$L_{NC} = a\Phi = a(2V)^{\frac{1}{3}}, \tag{28}$$

and hence

$$\frac{1}{[\sigma_{NC}(T)]_{\Delta U}^{\frac{1}{3}} \varrho_{t_F}} = a\left(2\frac{A_F^*}{\varrho_{t_F}}\right)^{\frac{1}{3}}. \tag{29}$$

By taking into account that $[\sigma_{NC}(T)]_{\Delta U}$ can be expressed by eq. (27), eq. (29) becomes

$$\varrho_{t_F} = \frac{1}{2^{\frac{1}{3}}\pi^{\frac{1}{3}} A_F^{*\frac{1}{3}} k^{\frac{1}{3}}} \frac{1}{a^{\frac{1}{3}}} \frac{1}{[r_{NC}(T)]_{\Delta U}^3}. \tag{30}$$

Now we assume that A_F^* may range between 25 and 100 and that $k = \varrho_t/\varrho_{t_F} = 1.2 \pm 0.1$. These assumptions, ample enough to encompass whatever reliable values for A_F^* and k, imply that

$$A_F^{*\frac{1}{3}} k^{\frac{2}{3}} \simeq 10.5 \pm 4.5 . \tag{31}$$

The uncertainty given in eq. (31) is certainly overestimated since A_F^* increases as a function of T, while k decreases *vs.* T.

The dependence of $[r_{NO}(T)]_{\Delta U}^{-3}$ on T according to eq. (25) is shown by the dashed lines drawn in fig. 4*a*) for $\Delta U = 8$ MeV and in fig. 4*b*) for $\Delta U = 16$ MeV. These curves are compared with the straight full lines which represent the T^3 dependences:

$$[r_{NO}(T)]^{-3} = 6.4 \cdot 10^{36} T^3 \tag{32}$$

in fig. 4*a*) and

$$[r_{NO}(T)]^{-3} = 8 \cdot 10^{35} T^3 \tag{33}$$

in fig. 4*b*).

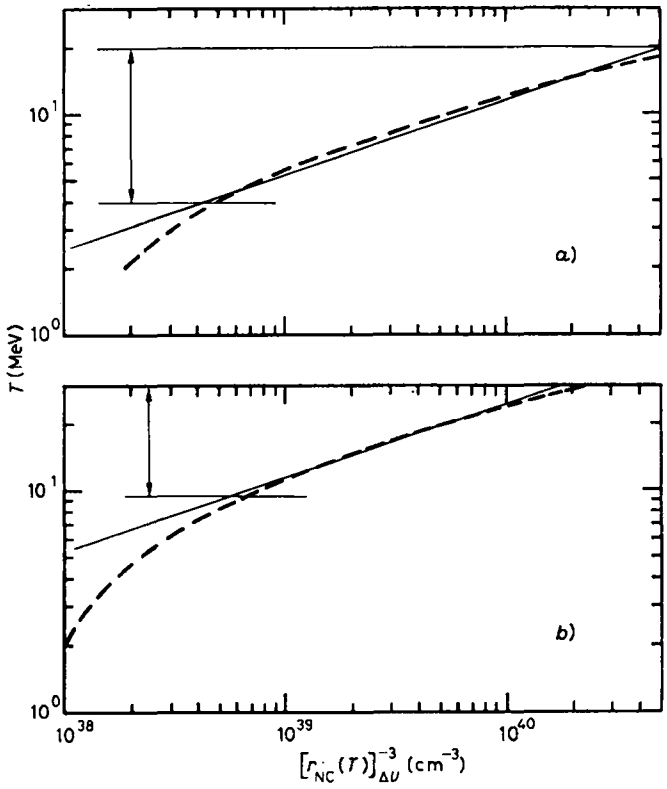

Fig. 4. – Dashed lines show the correlation between $[r_{NO}(T)]_{\Delta U}^{-3}$ and T which, according to eq. (25), is deduced for $\Delta U = 8$ MeV (*a*)) and for $\Delta U = 16$ MeV (*b*)). Full straight lines represent the equations $[r_{NO}(T)]^{-3} = 6.4 \cdot 10^{36}\, T^3$ (*a*)), $[r_{NO}(T)]^{-3} = 8 \cdot 10^{35}\, T^3$ (*b*)).

Figure 4*b*) shows that $[r_{NC}(T)]^{-3}_{\Delta U=16\text{MeV}}$ may be approximated by a T^3 dependence only in the temperature range $T = (10 \div 30)$ MeV. Since several points (T, ϱ_{t_F}) are located at $T < 10$ MeV (see fig. 3), the use of $[r_{NC}(T)]^{-3}_{\Delta U=16\text{MeV}}$ could not explain the whole observed dependence of ϱ_{t_F} on T.

Instead, the comparison made in fig. 4*a*) shows that $[r_{NC}(T)]^{-3}_{\Delta U=8\text{MeV}}$ can be well approximated by a T^3 dependence in the whole temperature range $T \simeq (4 \div 20)$ MeV, within which all evaluated points are located.

Also ϱ_{t_F}, according to eq. (19), exhibits an empirical dependence on T^3. This allows us to assume that the parameter a of eq. (30) can be considered constant for $\Delta U = 8$ MeV.

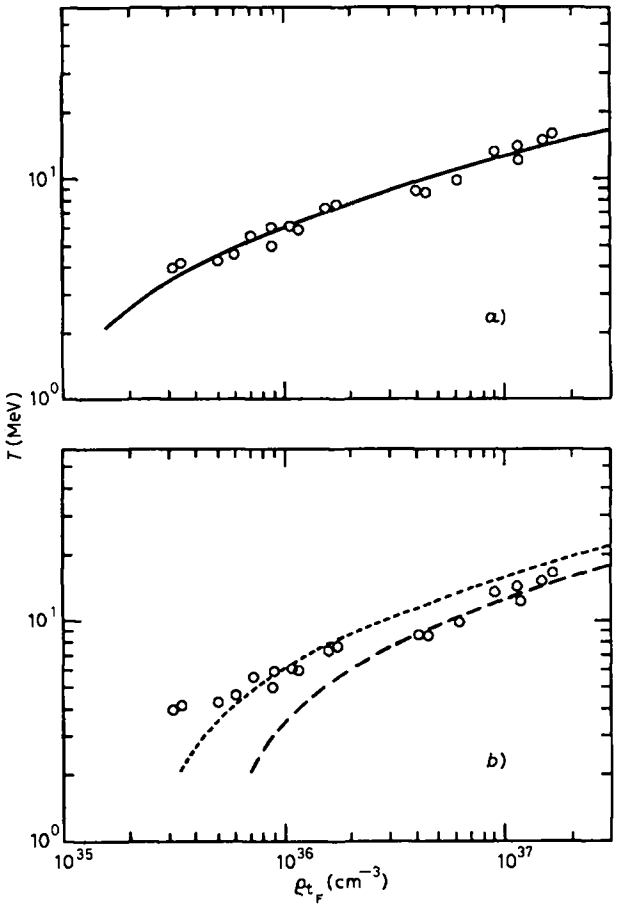

Fig. 5. – *a*) Comparison between the (T, ϱ_{t_F}) points evaluated by the present statistical approach (open circles) and expectations of the formulated model according to eq. (34) which adopts the value $\Delta U = 8$ MeV (full line). *b*) Two examples of comparisons, analogous to the one made in *a*), by using this time the value $\Delta U = 16$ MeV (dashed lines). These comparisons show that the assumption $\Delta U = 16$ MeV in eq. (30) cannot well explain the whole observed correlation between ϱ_{t_F} and T.

Finally, we have to ascertain whether eq. (30) yields also right quantitative values. To such a purpose we determine the parameter a in order to verify if it implies a P_{NF} value that satisfies the freeze-out conditions. To do it, we observe that the proportionality between ϱ_{t_F} and $[r_{NC}(T)]^{-3}_{\Delta v}$ expressed by eq. (30) allows us to translate along the abscissa axis the curves of fig. 4 which represent $[r_{NC}(T)]^{-3}_{\Delta v}$ until these curves fit in the best possible way the (T, ϱ_{t_F}) points. Such a translation is equivalent to determining the factor $1/2^{\frac{1}{2}}\pi^{\frac{3}{2}}A_F^{*\frac{1}{2}}k^{\frac{3}{2}}a^{\frac{3}{2}}$ of of eq. (30) and hence, in account of the value (31), the parameter a.

The points (T, ϱ_{t_F}) evaluated by using the statistical approach described in subsect. 3·2 and 3·5, shown in fig. 3, are also reported as circles in fig. 5*a*) and *b*). Two examples of $[r_{NC}(T)]^{-3}_{\Delta v=16\text{MeV}}$ translations parallel to the abscissa axis are considered in fig. 5*b*). As expected, according to our comments about fig. 4*b*), the inadequacy is evident of $[r_{NC}(T)]^{-3}_{\Delta v=16\text{MeV}}$ to yield the whole observed behaviour of ϱ_{t_F} as a function of T.

Instead, and coherently with what is observed in fig. 4*a*), fig. 5*a*) shows the remarkable agreement between eq. (30) and the (T, ϱ_{t_F}) point obtained through a suitable translation along the abscissa axis of $[r_{NC}(T)]^{-3}_{\Delta v=8\text{MeV}}$. The translation factor is deducible from eq. (30), by taking into account that $[r_{NC}(T)]^{-3}_{\Delta v=8\text{MeV}}$ and ϱ_{t_F} are both well approximated as a T^3 dependence by means of eqs. (32) and (19), respectively. Then

$$a^{\frac{3}{2}}(2^{\frac{1}{2}}\pi^{\frac{3}{2}}A_F^{*\frac{1}{2}}k^{\frac{3}{2}}) = \frac{[r_{NC}(T)]^{-3}_{\Delta v=8\text{MeV}}}{\varrho_{t_F}} = \frac{6.4\cdot 10^{36}\,T^3}{5.3\cdot 10^{33}\,T^3} = 1.2\cdot 10^3\,. \tag{34}$$

From eq. (34) we can finally deduce the parameter a. By using the value (31) into eq. (34), we obtain that $a^{\frac{3}{2}}$ may range between 9.6 and 24. Consequently, as shown in fig. 6, P_{NF} ranges between ~ 0.80 and ~ 0.89.

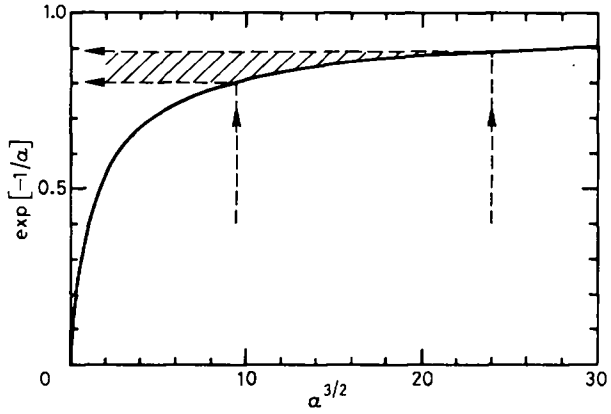

Fig. 6. – Probability $P_{NF} = \exp[-1/a]$ that nucleons do not suffer capture collisions, *vs.* $a^{\frac{3}{2}}$. Vertical arrows delimit the range of $a^{\frac{3}{2}}$ deduced by eq. (34) taking into account the value (31). Horizontal arrows and dashed area show the consequently deduced range of P_{NF}.

Remarkably, the range covered by P_{NF} satisfies, in practice, the real conditions required in order that the freeze-out stage take place. This result seems to give a good support to the reliability of the adopted model.

6. – Conclusions.

A new statistical approach is here adopted to evaluate temperature and free-nucleon densities of dilute nuclear matter (subsect. 3·1 and 3·2). Its application requires only the knowledge of suitably chosen yield ratios (subsect. 3·2 and 3·5) between different light composites emitted by a nuclear source hypothesized in the freeze-out stage.

Light clusters emitted in heavy-ion collisions can be considered unique in order to give information on the freeze-out stage (subsect. 2·1) and good messengers of a common piece of exploding nuclear matter (subsect. 3·2). These properties are not attributable to the nucleon emission.

The freeze-out stage, when it is reached, either directly or through different sequential steps, constitutes the last stage of the whole reaction mechanism involved in heavy-ion collisions (subsect. 2·1). The physical conditions which characterize this last stage are independent of the evolution of the excited nuclear matter (subsect. 5·3).

We evaluate temperature and free-nucleon densities of nuclear matter in the freeze-out stage under the assumption that both thermal and chemical equilibrium are reached (subsect. 3·1). Coherently with this assumption a careful selection of experimental data is made, when necessary (subsect. 3·5), in order to separate events attributable to the « equilibrium component » (subsect. 3·4).

Experimental data needed to apply the here proposed evaluation method are yield ratios between emitted composites differing either for a proton or for a neutron (subsect. 3·2). We use all known data about the ^{2}H, ^{3}H, ^{3}He, ^{4}He cluster emission since most of the available data concerning composite-particle emission in heavy-ion collisions are limited to the hydrogen and helium isotopes (subsect. 3·2). We exclude from our analysis the proton emission data for the reasons given in subsect. 3·2.

The more accurate estimates of T deduced by our analysis are obtained at lower temperatures (subsect. 3·2) just where the usual T estimates, deduced by fitting the energy spectra, may be affected by the largest uncertainties (subsect. 2·2). Then, the here adopted evaluation procedure can be considered particularly appropriate to evaluating temperatures T of equilibrated nuclear sources which decay with nonnegligible emission of light composites. In fact, the temperatures involved in such decays should not exceed some tens of MeV, since at higher temperatures the composite-particle production is strongly suppressed.

The here found values of temperature are limited between about 4 and

20 MeV, although the projectile energy per nucleon of the 19 investigated reactions covers about two orders of magnitude (table I). This result seems to confirm that the evaluation procedure and the treatment of data here adopted are actually appropriate to investigate the hypothesized nuclear systems. The high values of temperatures ranging up to the limiting temperature $T_{max} \simeq m_\pi c^2$ (subsect. **2**·2) concern to the free-nucleon and pion emission ([7,21,32]).

Another aspect we like to underline is the fact that the absolute values of the free-nucleon densities ϱ_{pF}, ϱ_{nF} and hence $\varrho_{tF} = \varrho_{pF} + \varrho_{nF}$ are deduced by the present analysis. The found values of ϱ_{tF}, ranging within two orders of magnitude (table I, fig. 3), show a dependence on T which can be well approximated by $\varrho_{tF} \simeq 5.3 \cdot 10^{33} T^3$ cm^{-3} (subsect. **4**·3).

We formulate a dilute-nuclear-matter model in order to deduce an approximate but quantitative interpretation of this empirical correlation. The basic points of the model (sect. **5**) may be summarized as follows:

a) Assumptions made about the constituents of the considered nuclear system are ample enough to encompass as much as possible its composition (subsect. **5**·1).

b) Nuclear-capture interactions are described by using a potential-energy–distance relation recently adopted to describe successfully different atomic, molecular, metallic and nuclear systems (subsect. **5**·1). This relation is based only on the two parameters r_0 and ΔU, which represent the equilibrium spacing and the equilibrium binding energy, respectively (subsect. **5**·1).

c) A capture radius $[r_{NC}(T)]_{\Delta U}$ weighted over the thermal-energy distribution of constituents is defined (eq. (25)). For radial distance below this radius, which is a function of both T and ΔU, the colliding nucleons are assumed to be captured in a bound state (subsect. **5**·2).

d) The freeze-out stage is determined by the probability P_{NF} that nucleons do not suffer capture collisions (subsect. **5**·3).

A remarkable quantitative agreement between expectations of the model (eq. (30)) and the empirical (T, ϱ_{tF}) correlation is obtained for $\Delta U = 8$ MeV. This agreement implies $P_{NF} = 0.8 \div 0.9$, which in our opinion satisfies in the best possible way the actual freeze-out conditions. The deduced value $\Delta U = 8$ MeV can be considered as a very reliable result since it is the most appropriate value to be expected when surface effects in finite nuclei are taken into account.

According to the model predictions (eq. (30)), the dependence of ϱ_{tF} on T, for $\Delta U = 8$ MeV, can be approximated by $\varrho_{tF} \simeq 5.3 \cdot 10^{33} T^3$ only for the temperature range, between $T \simeq 4$ MeV and $T \simeq 20$ MeV, which encompasses all the found (T, ϱ_{tF}) pairs. For other values of T the expected behaviour of ϱ_{tF} *vs.* T tends to deviate from the T^3 dependence (fig. 4). Temperatures higher

than ~ 20 MeV are expected to be concerned with nuclear regions exploding essentially into free nucleons and also pions at the higher temperatures. Lower temperatures might be concerned with nuclear systems decaying with nonnegligible emission of composites heavier than the light clusters here considered.

The good quantitative agreement between the found (T, ϱ_{t_F}) correlation and predictions of the adopted nuclear model seems to indicate that the adopted simplified assumptions may have real physical significance. We think that both new experiments and more sophisticated theoretical approaches are needed before definitively establishing the here found and interpreted correlation between T and ϱ_{t_F}.

● RIASSUNTO

Si adotta un nuovo approccio statistico che, mediante un'opportuna analisi delle particelle leggere emesse nelle reazioni tra ioni pesanti, permette di calcolare le densità dei nucleoni liberi e la temperatura della sorgente di emissione. Si usano tutti i dati noti riguardanti l'emissione di ^{2}H, ^{3}H, ^{3}He, ^{4}He misurati in un unico esperimento. Questi dati si riferiscono a 19 reazioni tra ioni pesanti studiate a energie comprese tra 26 e 2100 MeV per nucleone. Gli eventi analizzati sono soltanto quelli che, mediante accurate selezioni, possono essere attribuiti alla componente di equilibrio. Tra i risultati, si osserva una correlazione tra la densità totale dei nucleoni liberi ϱ_{t_F} e la temperatura T della sorgente. Si formula un modello della materia nucleare per confrontare le previsioni quantitative di tale modello con la correlazione osservata tra T e ϱ_{t_F}. Questo confronto dà un accordo soddisfacente.

Резюме не получено.